

Resource Allocation for Video Streaming in Multi-User Wireless Networks

by

Sabarna Choudhuri

A Thesis Presented in Partial Fulfillment
of the Requirement for the Degree
Master of Science

Approved June 2014 by the
Graduate Supervisory Committee:

Lei Ying, Chair
Daniel Bliss
Martin Reisslein

·
·

ARIZONA STATE UNIVERSITY

August 2014

ABSTRACT

Survey indicates a rise of 81% in mobile data usage in the year 2013. A fair share of this total data demand can be attributed to video streaming. The encoding structure of videos, introduces nuances that can be utilized to ensure a fair and optimal means of streaming the video data. This dissertation proposes a novel user and packet scheduling algorithm that guarantees a fair allocation of resources. MS-SSIM index is used to calculate the mean opinion score (DMOS) to evaluate the quality of the received video. Simulations indicate that the proposed algorithm outperforms existing algorithms in the literature.

to ma and baba...

ACKNOWLEDGEMENTS

First and foremost I would like to express my deep gratitude to my advisor Dr .Lei Ying for being an endless source of inspiration and motivation to pursue research in Theoretical communications. He has been most kind and understanding as an advisor. I am sincerely thankful and indebted for his patience and guidance throughout my research.

I would like to thank my committee member Dr .Dan Bliss for giving me the opportunity to be a part of his project on Channel Estimation using Software Defined Radio. His class on Spectral Estimation was one of the most interesting classes I have attended during my Masters at ASU. He has also been very generous in letting me work on highly interesting projects using USRPs.

I am thankful and honored to have Dr .Martin Reisslein preside over my Thesis defense as a committee member. Much of my knowledge on Video transmission was obtained from his papers on Network performance evaluation using MPEG-4 and H.263 video traces.

I would also like to thank Weina Wang for her help and guidance during my research.

My parents Mr. Nemaï Choudhuri and Mrs. Sakuntala Choudhuri, to whom I dedicate my work, have been a constant source of support throughout the two years I have spent away from home. Their dedication and unconditional love is one of the major reasons behind the successful completion of this dissertation. I am also grateful to my sisters Dr. Satarupa Choudhuri and Dr. Samadrita Choudhuri who have gone out of their way to help and support me at times of need.

I am also thankful to all my friends and seniors who have been extremely kind and helpful during my stay at Arizona.

TABLE OF CONTENTS

	Page
LIST OF TABLES	vi
LIST OF FIGURES	vii
CHAPTER	
1 INTRODUCTION	1
1.1 Research Motivation and Contributions	2
1.2 Related Work	2
2 VIDEO CODEC CONFIGURATION AND PLAYOUT STRUCTURE ..	4
2.1 Scalable Video Coding	4
2.2 Basics of H.264/AVC	6
2.2.1 Network Abstraction Layer	6
2.2.2 Video Coding Layer	6
2.3 SVC extension to H.264/AVC	7
2.3.1 Temporal Scalability	7
2.3.2 Spatial Scalability	9
2.3.3 Quality Scalability	10
2.4 Rate Distortion Model	12
2.5 Playout Model	12
3 SYSTEM MODEL	14
4 USER SELECTION ALGORITHM	15
4.1 Capacity Region	15
4.2 Problem Formulation	16
4.3 User Selection Algorithm	17
5 PACKET SCHEDULING ALGORITHM	19
5.1 Layer selection	19

CHAPTER	Page
5.2 Packet Scheduling Algorithm	19
5.3 Optimality of the Packet Scheduling Algorithm	20
6 SIMULATIONS AND RESULTS	27
6.1 Channel Model	27
6.2 Performance Evaluation	29
7 CONCLUSIONS AND FUTURE WORK	33
7.1 Conclusion	33
7.2 Future Work	33
REFERENCES	34

LIST OF TABLES

Table	Page
6.1 DMOS Scores.....	31

LIST OF FIGURES

Figure	Page
2.1 Spatial Scalability	5
2.2 Temporal Scalability	5
2.3 Quality Scalability	5
2.4 IBBP prediction structure	7
2.5 Hierarchical B prediction structure	8
2.6 Nondyadic hierarchical prediction structure	8
2.7 Hierarchical prediction structure with zero encoding/decoding delay ...	9
2.8 Spatial Scalability	10
2.9 Base Layer only control	10
2.10 Enhancement Layer only control	11
2.11 Hierarchical prediction structure of SVC	11
2.12 Rate Distortion Graph	12
2.13 Playout Structure	13
3.1 Wireless System Model	14
6.1 Logarithm of Throughput of User 1	29
6.2 Logarithm of Throughput of User 2	29
6.3 Logarithm of Throughput of User 3	30
6.4 Screen shot of the reconstructed video for User 3 under Congestion Control Policy	31
6.5 Screen shot of the reconstructed video for User 3 under Heuristic 1	31
6.6 Screen shot of the reconstructed video for User 3 under Heuristic 2	32

Chapter 1

INTRODUCTION

Content delivery systems have evolved a long way from playing elevator music in the early 1930s to live streaming of videos at user end devices. The advent mobile networks have resulted in the rise of demand in multimedia content being delivered at a reasonable cost and quality. It is therefore essential to develop algorithms that facilitate the efficient utilization of spectral resources and deliver a fair and acceptable quality of media stream.

Previous video coding standards such as MPEG-2, H.263, or MPEG-4 Part 2 failed to provide the granularity in service without unnecessary rise in complexity of devices. A major breakthrough was provided by the H.264 SVC extension. By constructing sub-bitstreams out of the original bitstream, SVC is able to provide multiple standards of viewing quality, thereby changing the traditional concept of being able to view or not being able to view a video content. Moreover it also incorporates in its design a base layer bitstream that is fully capable of being decoded by a standard H.264 AVC decoder without the SVC extension. A typical H.264 video decoder consists of the following functional blocks.

Motion estimation: Identify temporal and spatial redundancies between individual frames and encodes successive frames based on these redundancies.

Transform: Perform transformation from spatial to frequency domain, typically using a DCT 4×4 transform.

Quantization: Quantize the coefficients from the transform stage, maintaining an acceptable quality of Video.

Entropy coding: Serialize the 4×4 quantized coefficients using a scan pattern that orders the coefficients from low frequency to high frequency.

1.1 Research Motivation and Contributions

The scalability of H.264 encoding format quite naturally necessitates the utilization of efficient algorithms that are capable of selectively encoding the video depending on the channel quality. When serving a set of users on a slotted system a natural question of user selection arises. The objective is to grant each of the users a fair and acceptable viewing quality based on their channel conditions. This also leads to the question of efficiently constructing bitstreams for a user such that the total bitrate is within the channel capacity. The contributions of this thesis are as follows:

1. An user scheduling algorithm that provides a fair and acceptable viewing quality to all the users and maximize the sum of user utilities.
2. A threshold based packet scheduling algorithm that provides a minimum threshold viewing quality to all the users, where the threshold values are determined by the user scheduling algorithm. .
3. Evaluation of the user and packet scheduling algorithm on real videos from the LIVE database (<http://live.ece.utexas.edu/research/quality/subjective.htm>) using DMOS scores.

1.2 Related Work

In Chen *et al.* (2012) the problem of adaptive data scheduling is dealt as a sequential decision problem. The buffer state and the channel dynamics have been modeled using a Markov chain and Markov Decision Process is used to study the scheduling methods. In Maani *et al.* (2007) scheduling policy attempts to minimize the expected distortion greedily for a given number of bits. In Hassan *et al.* (2008) a heuristic

is proposed that maintains a queue for each priority group, taking into account the delay and priority of the buffer state along with the channel condition, is proposed. The optimization of transmitter rate in order to optimize quality for single stream has been studied in Chou and Miao (2006) and Lu *et al.* (2007). In Ferrari and Verma (1990) users are assumed to have similar channel dynamics. In Cheng *et al.* (2006) FGS coding is utilized to provide a constant video quality. However packet losses are not considered. In Costa *et al.* (2004) base layers are assumed to be delivered without any loss.

Chapter 2

VIDEO CODEC CONFIGURATION AND PLAYOUT STRUCTURE

2.1 Scalable Video Coding

In general scalability entails the original stream to be removed in such a way that resulting substreams form a valid bitstream. This bitstream will yield a reconstructed quality less than the original bitstream. Detailed versions of the following sections can be found in Schwarz *et al.* (2007). Prior to the Scalable Video Coding feature of H.264, video coding standards such as H.262 MPEG-2 Video, H.263 and MPEG-4 Visual provided means to support scalability. However spatial and quality scalability features of those standards accompanied significant loss in coding efficiency and increase in decoder complexity.

Scalable coding is usually classified into spatial, temporal, quality scalability. Spatial scalability results in a reduced picture size, temporal scalability implies reduced frame rate and quality scalability, although provides the same spatio-temporal resolution as the original bitstream, results in a lower fidelity. It is analogically related to the SNR of the original bitstream. Region of interest based scalable modes are available that generate substreams based on spatially contiguous regions of the original picture area. Different types of scalability are also often combined.

Examples of spatial, temporal and quality scalability are illustrated in the following figures.



Figure 2.1: Spatial Scalability

1

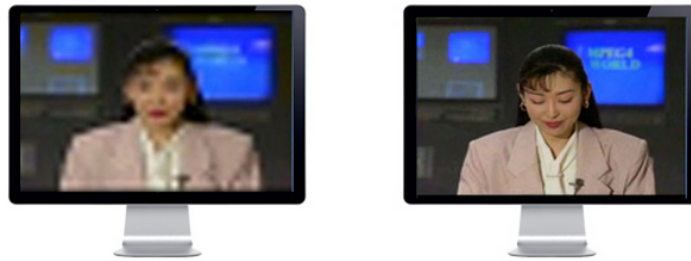


Figure 2.2: Temporal Scalability

2



Figure 2.3: Quality Scalability

3

2.2 Basics of H.264/AVC

H.264 design entails two layers the Video Coding Layer(VCL) and the Network Abstraction Layer(NAL). The coded version of the source content is created by the VCL. Formatting of this data and header information is provided by the NAL.

2.2.1 Network Abstraction Layer

After coding the video data, they are organized into packets containing integer number of bytes .These packets are called NAL units. It starts with a 1 byte header that indicates the type of data contained. The payload of the packet consists of the remaining bytes. The NAL units are classified into the VCL NAL units and the non-VCL NAL units. The VCL NAL unit consists of coded slices and the non VCL NAL units consist of parameter sets and Supplemental Enhancement Information (SEI).SEI messages are used to decode information and bit stream manipulation.

2.2.2 Video Coding Layer

Pictures are partitioned into smaller coding units into macroblocks and slices. A macroblock consists of a rectangular area of 16×16 luma samples and for videos in 4:2:0 chroma sampling format, 8×8 samples of each of the two chroma components. Spatial or temporal prediction methods are used to predict the samples and the residual signals are represented using transform coding. Macroblocks are organized into slices that can be parsed independently. H.264/AVC supports three slice coding types:

I: Uses intra-picture predictive coding

P: Uses intra-picture predictive and inter-picture coding

B: A weighted average of Intra-picture, Inter-picture and Inter-picture bipredictive

coding is used.

Figure 2.4 shows the various prediction structures.

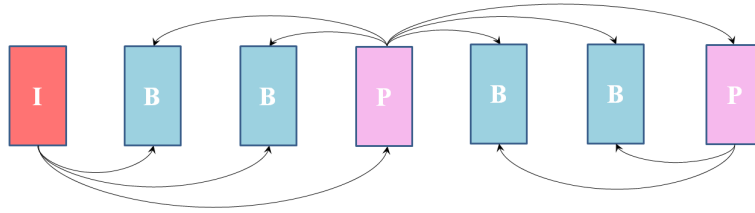


Figure 2.4: IBBP prediction structure

2.3 SVC extension to H.264/AVC

As discussed before scalability can be of three primary types. Temporal scalability, Spatial scalability and Quality scalability.

2.3.1 Temporal Scalability

Here the coded units are partitioned into a temporal base layer and one or more enhancement layers. As shown in Figures 2.5-2.7, the temporal layer identifier T_0 indicates the temporal base layer. For any natural number k a valid bitstream can be formed by removing all the layers $T_{k'}$ such that $k' > k$.

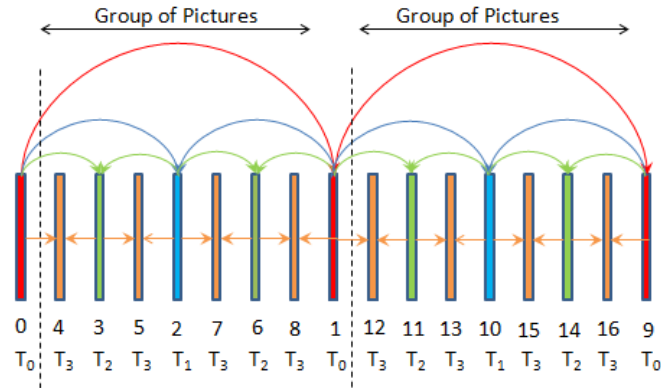


Figure 2.5: Hierarchical B prediction structure

Figure 2.5 shows a typical dyadic prediction structure where I layers are only predicted from previous I layers. Other layers are predicted from the nearest lower temporal layers from the past and future.

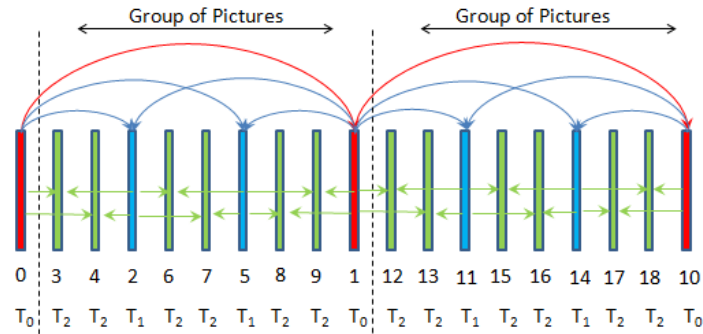


Figure 2.6: Nondyadic hierarchical prediction structure

Figure 2.6 shows a nondyadic hierarchical prediction structure with 2 independently decodable subsequences that provides 1/9th and 1/3rd of the full frame rate.

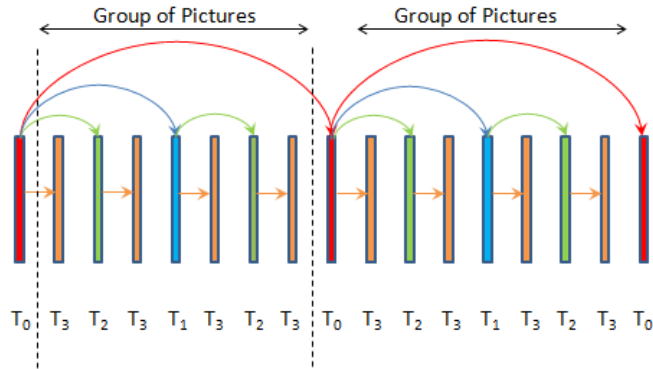


Figure 2.7: Hierarchical prediction structure with zero encoding/decoding delay

Figure 2.7 shows a prediction structure that does not utilize motion compensation from pictures in the future, thereby yielding a zero encoder/decoder delay. Quantization parameters chosen for the pictures belonging to different temporal layers greatly affect the coding efficiency. Temporal base layer is coded with very high fidelity. For following temporal layers large quantization parameters can be chosen.

2.3.2 Spatial Scalability

Spatial resolution as described before is utilized in Spatial Scalability. Different spatial resolutions are ordered in the increasing order of their spatial resolution. Intraprediction and motion-compensated prediction is used for single layer coding. Spatial scalability is shown in Figure 2.8

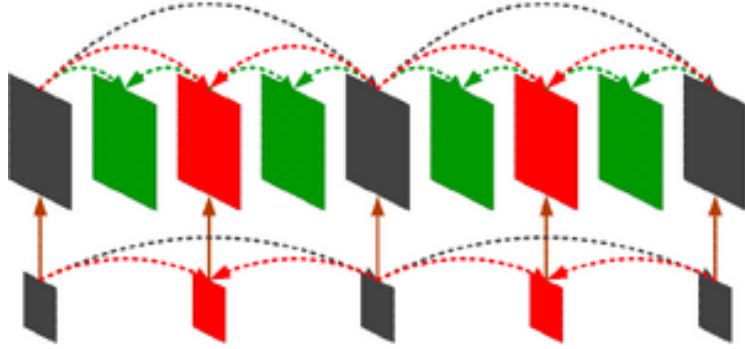


Figure 2.8: Spatial Scalability

2.3.3 Quality Scalability

Like in Spatial scalability same picture sizes are used for the base and the enhancement layer. Interlayer prediction is used for coarse grain scalability in SVC. To increase flexibility of bitstream adapting and error robustness MGS approach is used which allow further fine tuning of the choices of the layers to be transmitted.

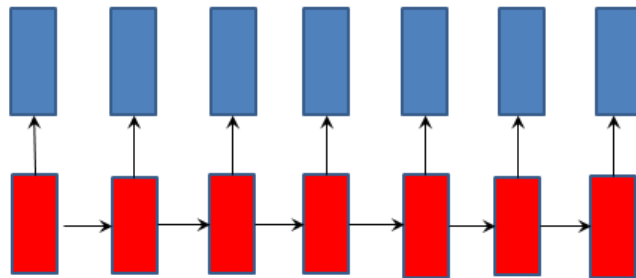


Figure 2.9: Base Layer only control

Figure 2.9 shows a structural decoding scheme with Base layer only control.

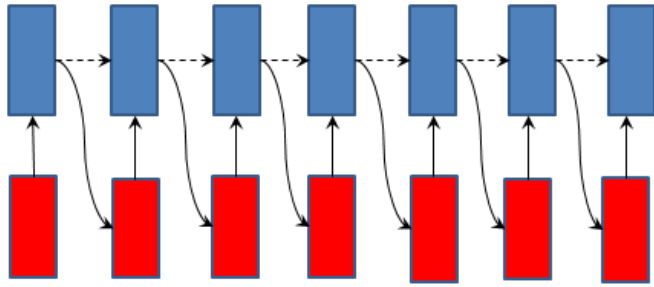


Figure 2.10: Enhancement Layer only control

Fig 2.10 shows a scheme with enhancement layer only control.

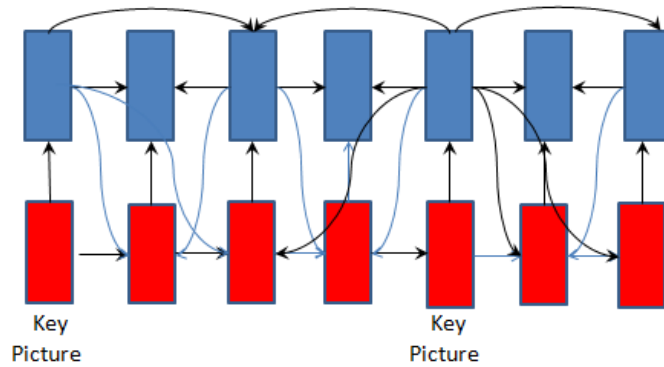


Figure 2.11: Hierarchical prediction structure of SVC

Figure 2.11 shows hierarchical prediction structure of SVC.

The various advantages of scalable video coding can be listed as follows:

1. For clients with heterogeneous channel conditions there could be one primary source bitstream with highest resolution and scalable bitstreams of lower resolutions can be obtained out of it by discarding selected data.
2. Unequal error protection could be granted to parts of the video that may have crucial application and parts of the video can be decoded with high quality.
3. For each subset of the scalable video coding efficiency is the same as single layer

coding.

4. Scalable video coding is of great use for video surveillance operations.

2.4 Rate Distortion Model

The Rate distortion model in our analysis is same as the one proposed in Chen *et al.* (2012). If q_f is the amount of data contained by a frame f , $d_f(q_f)$ gives the quality when q_f is decoded. Only when 0 to $l-1$ layers have been successfully received $w_{f,l}$ can be successfully decoded, where $w_{f,l}$ denotes the amount of data contained in the $(f, l)^{th}$ layer. Distortion is a right continuous function with jumps at every time a new data packet is successfully decoded.

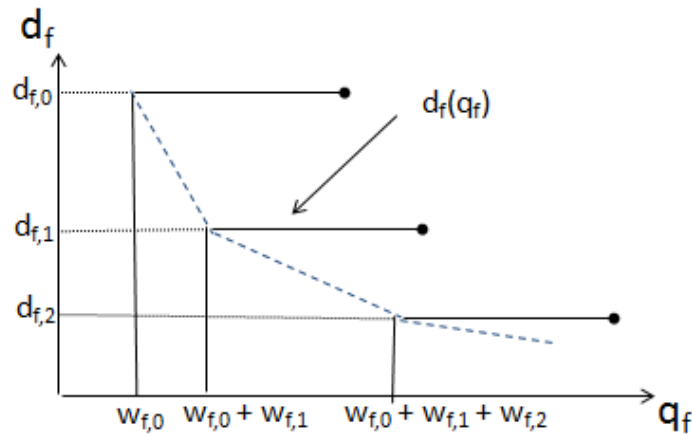


Figure 2.12: Rate Distortion Graph

2.5 Playout Model

The playout model followed at the receiver end is described in Fig 2.14. The packets on the left side of the y-axis indicates that those packets have been played out. The packet indices are ordered as (m,n) where m indicates the order of the frame in time and n indicates the layer of the frame. The first frame due for playing

is called the current frame. The expired frames are indicated with negative indices. The playout follows the prediction structure, i.e. the base layer $(m,0)$ needs to be received to be successfully before $(m,1)$ or $(m,2)$ could be decoded. Also the I frame (key picture) needs to be received before transmitting the B or P frames.

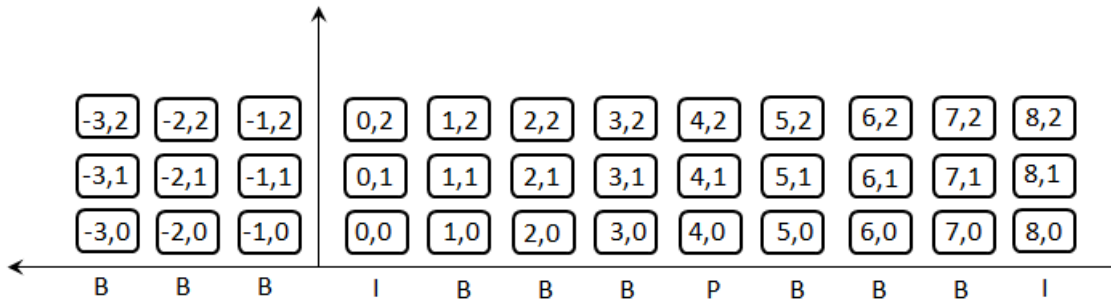


Figure 2.13: Playout Structure

Chapter 3

SYSTEM MODEL

In this setting a set of N users are being considered for transmission of a single stored video from a single server. We consider a time slotted system, where at each time slot t , the server chooses a user for transmission of video data packets. These packets correspond to the individual layers pertaining to the video frames. A buffer maintained at the receiver end keeps track of the received packets. A Group of frames (GOP) get decoded together and at each timeslot t a decoded frame is played out at the receiving user equipment. When a GOP gets decoded its un-received frames are dropped.

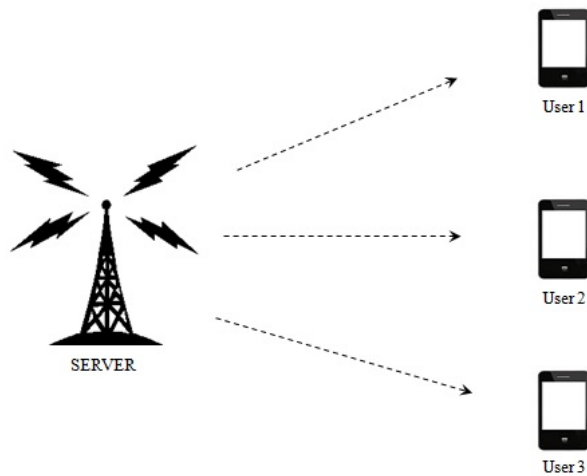


Figure 3.1: Wireless System Model

USER SELECTION ALGORITHM

The utility of user selection algorithms is to support any traffic within the capacity region. However, in practical scenarios user selection algorithms are often influenced by scheduling algorithms, especially the ones that influence transmission rates based on queue state of individual users. Therefore in the following proposal we introduce a joint congestion control and scheduling algorithm that maximizes our objective function. The theory is covered in detail in R.Srikant and Ying (2013)

4.1 Capacity Region

We consider a total of M possible channel states. Let μ_m be the transmission rate of the server, to any particular user, at channel state m . We denote the fraction of time user n gets allocated in channel state m as $\alpha_{m,n}$, where

$$\sum_n \alpha_{m,n} = 1$$

Therefore the actual data rate obtained by user n in channel state m is given as

$$r_{m,n} = \alpha_{m,n} \times \mu_m$$

If π_m is the fraction of time channel is in state m such that ,

$$\sum_{1 \leq m \leq M} \pi_m = 1$$

then the achievable data rate for user n is

$$r_n = \sum_m \pi_m r_{m,n} = \sum_m \pi_m \alpha_{m,n} \mu_m$$

We define the Capacity region \mathcal{C} as the set of all such achievable rates for a given channel state m

$$i.e., \mathcal{C} = \{r : r = \alpha_{m,n} \mu_m \text{ such that } \sum_n \alpha_{m,n} = 1\}$$

4.2 Problem Formulation

In this problem Video Quality at the user equipment is characterized as a strictly concave function of user throughput. All stationary variables are indicated by the absence of the function t .

Notations:

p_n : Average throughput for user n

$f(\cdot)$: Concave quality function Therefore for p_n packets, the average decoded quality is given as $f(p_n)$

We define a minimum Threshold Video Quality which our algorithm strives to provide to each user.

$p_{th,n}$: Average throughput corresponding to Threshold quality, for user n such that ,

$$p_n > p_{th,n}$$

The objective of the optimization algorithm is to provide all users with the minimum threshold quality of $f_{th,n}$ where

$$f_{th,n} = f(p_{th,n})$$

The optimization problem is framed as :

$$\begin{aligned} & \underset{f_{th}}{max} && \sum_n f_{th,n} \\ & \text{subject to} && p_n > p_{th,n} \text{ for all } n \\ & && p_n \in \mathcal{C} \end{aligned}$$

In order to provide a fair resource allocation we choose our utility function to be $\log(p_{th,n})$.

From the above Optimization problem we formulate the following Lagrangian

$$\mathcal{L} = \max \sum_n f_{th,n} + \sum_n \lambda_n (p_n - p_{th,n})$$

where λ_n is the Lagrangian multiplier.

4.3 User Selection Algorithm

For a fixed λ_n , the Lagrangian can be decomposed into two problems as follows,

Problem 1:

$$\max \sum_n f_{th,n} - \sum_n \lambda_n p_{th,n}$$

Problem 2:

$$\max \lambda_n p_n$$

At each timeslot t the server selects an user based for transmission of data packets. Three parameters are used to govern the User selection at timeslot t . The congestion control parameter, the virtual queue and the channel throughput, all of which are evaluated at every timeslot.

The Congestion Control parameter is the solution of Problem 1, the Congestion Control Algorithm

$$\max \sum_n f_{th,n} - \sum_n \lambda_n p_{th,n}$$

At every timeslot the value of the throughput threshold is derived as

$$p_{th,n}(t+1) = (p_{th,n}(t) + \delta(\frac{1}{p_{th,n}(t)} - \lambda_n(t)))^+$$

Further inspection shows that the Lagrangian parameter obeys the dynamics of a queue. This virtual queue is utilized to keep a track of deficit in service. From the Lagrangian formulation we have

$$\max \sum_n \lambda_n p_n$$

Using the queue interpretation of the Lagrangian multiplier we arrive to the following Scheduling Algorithm.

$$u(t) = \operatorname{argmax}_n q_n \mu_n$$

where $u(t)$ is the user to be Scheduled at timeslot t . At timeslot $(t+1)$ the virtual queue is updated as

$$q_n(t+1) = (q_n(t) + p_{th,n}(t) - \mu_n(t))^+$$

PACKET SCHEDULING ALGORITHM

5.1 Layer selection

At each timeslot t the server chooses packets pertaining to various layers. We follow a couple of basic assumptions while transmitting packets to individual users.

Assumptions:

1. Layers pertaining to only those frames are selected that have not been decoded.
2. The enhancement layer of a frame is scheduled for transmission only after the base layer of the frame is received.
3. The base layer of a frame is scheduled after the base layer of its reference frame is scheduled.

Our Layer Selection policy is motivated from solving the MDP based policy proposed in Chen *et al.* (2012). For each frame to be transmitted the first l layers are selected, starting from the base layer. The value of l is decided by the threshold rate (derived from the congestion control algorithm) and the channel rate for that time slot. i.e. If $\xi(l)$ is the amount of data in the first l layers of a frame to be transmitted.

$$\xi(l) = \min(p_{th}, \mu)$$

5.2 Packet Scheduling Algorithm

In order to provide optimal video quality to all the users we propose an algorithm that aims at providing a fixed threshold number of packets for each frame. The Threshold value for each frame is decided by the congestion control parameter $P_{th,n}(t)$ (number of packets pertaining to the Threshold rate $p_{th,n}(t) / c_n(t)$), which

is calculated at every timeslot t . Our Algorithm states that if $\mathcal{P}_i^n(t)$ denotes the number of packets to be served for each frame in the i^{th} group of pictures of user n at timeslot t and $i\tau$ be the time by which the i^{th} Group of Pictures are decoded

$$\begin{aligned}\mathcal{P}_i^n(t) &\leq P_{th,n}(t) \\ \mathcal{P}_i^n(t) &= 0, t > i\tau\end{aligned}$$

5.3 Optimality of the Packet Scheduling Algorithm

Theorem 1. *For any given ϵ , for a set of users utilizing the user and packet Scheduling Algorithm described above*

$$E[f_n] \geq f_{th,n} - \epsilon$$

where f_n is the actual video quality obtained by user n

Proof. We consider a Bernoulli On/Off channel with probability of successful transmission \mathbf{P}_s in each timeslot.

Notations:

\mathbf{P}_{th} :- Number of packets corresponding to the threshold quality f_{th} for each frame.

P_{th} is chosen such that $P_{th} < P_s$.

\mathbf{T} :-Total number of timeslots/frames in each Group of frames.

We define our capacity region as all those rates of service that can be supported by the channel

$$\mathcal{C} = \{\tilde{P} | \tilde{P} \leq P_s\}$$

where, \tilde{P} :- Number of packets delivered in one timeslot.

We group I Groups of frames (GOF) to form an Interval and K such Intervals to form a Group of Intervals (GOI) . We define set $l = \{ I \text{ intervals} : P_{k_{ac}}TI < P_{th}TI \}$ and $L = |l|$. Considering the number of packets delivered in an I interval to be integers

$P_{k_{ac}}TI \leq P_{th}TI - 1 \quad \forall l \in L$. From Lemma 1 we have

$$\begin{aligned}
P_{th,n}T(K-1)I &\leq L(P_{th,n}TI - 1) + (K-L)P_{th,n}TI \\
\Rightarrow L &\leq P_{th,n}TI \\
\Rightarrow K-L &\geq K - P_{th,n}TI \\
\Rightarrow \frac{(K-L)I}{KI} &> \frac{K - P_{th,n}TI}{K}
\end{aligned}$$

Now for every frame, number of packets transmitted corresponds to the Threshold Quality and since quality is additive with respect to the number of packets we can multiply the Threshold quality f_{th} on both sides of the equation to obtain

$$\Rightarrow f_{th,n} \frac{(K-L)I}{KI} > f_{th,n} \frac{K - P_{th,n}TI}{K}$$

Let there exist an ϵ such that

$$\begin{aligned}
K &\geq \frac{f_{th,n}P_{th,n}}{\epsilon} \\
\Rightarrow \frac{f_{th,n}P_{th,n}}{K} &\leq \epsilon \\
\Rightarrow f_{th,n} \frac{(K-L)I}{KI} &> f_{th} - \epsilon
\end{aligned}$$

The total quality achieved by user n is $f_{th,n}(K-L)$. We denote this as f_n . For a large value of K, we have, by the Strong law of large numbers

$$E[f_n] \geq |f_{th,n} - \epsilon|$$

□

Lemma 1.

$$P_{th,n}T(K-1)I \leq L(P_{th,n}TI - 1) + (K-L)P_{th,n}TI$$

Proof. In order to prove the above inequality we propose a Delay policy that does not transmit packets pertaining to frames belonging to the first interval. It starts

transmission from the second I interval. If \mathcal{A} is the set of all frames belonging to the first interval Delay Policy can be defined as,

$$\mathcal{P}_i^n(t) \leq c_n(t) \text{ for } t \leq i\tau$$

$$\mathcal{P}_i^n(t) = 0 \text{ for } t > i\tau$$

$$\mathcal{P}_i^n(t) = 0 \forall i \in \mathcal{A}$$

We prove the above Lemma by induction.

Notation:

A_i^{pol} = Number of packets belonging from the 1st to the i^{th} Group of Pictures under our policy.

a_i^{pol} = Number of packets belonging to the i^{th} Group of Pictures under our policy.

B_i^{pol} = Number of packets successfully transmitted from timeslot 1 to timeslot iT under our policy

A_i^d = Number of packets belonging from the 1st to the i^{th} Group of frames under the delayed policy.

B_i^d = Number of packets successfully transmitted from timeslot 1 to timeslot iT under the delayed policy

- Statement: $A_j^{pol} \geq (j - I)P_{th,n}T$

- **Initial Step** When $j=I$

$$A_j^{pol} \geq 0$$

- **Inductive Step** If for any GOF $l \geq I$,

$$A_l^{pol} \geq (l - I)P_{th,n}T, \text{ then for } (l + 1)^{th} \text{ GOF}$$

$A_{l+1}^{pol} \geq (l + 1 - I)P_{th,n}T$ This can be established by enumerating the two possible cases,

Case 1: When $a_{l+1}^{pol} \geq P_{th,n}T$

$$A_{l+1}^{pol} = A_l^{pol} + a_{l+1}^{pol} \geq (l+1-I)TP_{th,n}$$

Case 2: When $a_{l+1}^{pol} < P_{th,n}T$

Since for the $(l+1)^{th}$ GOP, Threshold number of packets are not received, from the definition of our policy

$$\begin{aligned} A_{l+1}^{pol} &= B_{l+1}^{pol} \\ &= B_{l+1}^d \\ &\geq B_{l_0-1}^d \text{ for any } l_0, \text{ such that } l_0 = \left\lfloor \frac{l}{I} \right\rfloor + 1 \end{aligned}$$

Also, since $l+1$ and l_0 belong are GOPs belonging to the same interval $(l+1) - l_0 \leq I - 1$ From Lemma 2,

$$\begin{aligned} (l_0 - 1)P_{th,n}T &\leq B_{l_0-1}^d \\ \Rightarrow (l+1-I)P_{th,n}T &\leq B_{l_0-1}^d \\ &\leq B_{l+1}^d \\ &= B_{l+1}^{pol} \text{ since we assume the same channel dynamics} \\ &= A_{l+1}^{pol} \end{aligned}$$

- **Final Step** $A_i^{pol} \geq (j-I)P_{th,n}T$

Therefore for $(K-1)$ intervals the total number of packets delivered by our policy is greater than the threshold number of packets for $(K-1)$ intervals

$$\text{i.e. } P_{th,n}T(K-1)I \leq L(P_{th,n}TI - 1) + (K-L)P_{th,n}TI$$

□

Lemma 2. *The service rate of any user n , under our scheduling algorithm, converges to a Normal Distribution. i.e. For any $\sigma_P^2 \in [0, \infty)$ and $\sigma_P^2 > 0$ and any initial*

distribution π the service rate P , of a single user, obeys the Central Limit Theorem.

$$(\bar{P}_t - E_\pi P) \xrightarrow{d} N(0, \frac{\sigma_P^2}{\sqrt{t}})$$

Proof. The positive recurrence of the system X constituted by the queue ($q(t)$) and channel ($c(t)$) has been established in Lemma 4. We construct a function $P : X \rightarrow R$ such that $P(x)$ is the number of packets served in each time interval and $P^2(x) < (\frac{1}{2} \sum_i q^2(t))^2 + K$, where K is a constant. Then by Jones (2004) the function P obeys the Central limit theorem. Therefore,

$$(\bar{P}_t - E_\pi P) \xrightarrow{d} N(0, \frac{\sigma_P^2}{\sqrt{t}})$$

Now if Pk_{aci} be the number of packets transmitted for frame i by our policy

$$\sum_{n=1}^N \sum_{i=1}^{TI} Pk_{ac_i,n} \geq \sum_{n=1}^N P_{th,n} TI$$

holds with a very high probability. □

Lemma 3. *The system state X consisting of the channel state $\mu(t)$, queue state $q(t)$ is a Positive Recurrent Markov Chain*

Proof. Our system state can be modeled by taking the channel state $\mu(t)$, queue state $q(t)$ into account .

$$i.e. S(t) = \{q(t), \mu(t)\}_{t \in \mathbb{N}}$$

In order to show the stability of the queue it is essential to establish its positive recurrence , which is shown as following.

We know the queue evolves as

$$q_n(t+1) = (q_n(t) + c_n(t) - \mu_n(t))^+$$

Consider the Lyapunov function

$$V(t) \triangleq \frac{1}{2} \sum_i q^2(t)$$

The drift is given as

$$\begin{aligned}
& E[V(q(t+1)) - V(q(t)) | q(t) = q] \\
&= \frac{1}{2} E[\sum_i q_i^2(t+1) - q_i^2(t) | q(t) = q] \\
&= \frac{1}{2} E[\sum_i ((q_i(t) + c_i(t) - \mu_i(t))^+)^2 - q_i^2(t) | q(t) = q] \\
&\leq \frac{1}{2} E[\sum_i (q_i(t) + c_i - \mu_i(t))^2 - q_i^2(t) | q(t) = q] \\
&= \frac{1}{2} E[\sum_i (c_i(t) - \mu_i(t))^2 - 2q_i(t)(a_i(t) - \mu(t)) | q(t) = q] \\
&\leq K_1 + \sum_i q_i \bar{c}_i - \sum_i q_i \bar{\mu}_i
\end{aligned}$$

We assume $E[c_i^2(t)] \leq \sigma_{max}^2$ and $K_1 = \frac{N(\sigma_{max}^2 + \mu_{max}^2)}{2}$. By adding and subtracting with $\frac{1}{\epsilon} \sum_i U_i(\bar{c}_i)$ we get,

$$\begin{aligned}
& E[V(t+1) - V(t) | q(t) = q] \\
&\leq K_1 + \sum_i q_i \bar{c}_i - \frac{1}{\epsilon} \sum_i U_i(x_i(t)) + \frac{1}{\epsilon} \sum_i U_i(x_i(t)) - \sum_i q_i \bar{\mu}_i
\end{aligned}$$

We know $\bar{c}_i(t)$ maximizes $U_i(\bar{c} - \epsilon q_i \bar{c})$. Denoting this optimal value as c_i^* , we have

$$\frac{1}{\epsilon} U_i(c_i^*(1 - \delta)) - q_i c_i^*(1 - \delta) \leq \frac{1}{\epsilon} U_i(c_i(t)) - q_i c_i(t)$$

where $0 \leq \delta < 1$. Therefore we have,

$$\begin{aligned}
& E[V(t+1) - V(t) | q(t) = q] \\
&\leq K_1 + \sum_i q_i c_i^*(1 - \delta) - \frac{1}{\epsilon} \sum_i U_i(c_i^*(1 - \delta)) \\
&\quad + \frac{1}{\epsilon} \sum_i U_i(x_i(t)) - \sum_i q_i \bar{\mu}_i \\
&= K_1 + \sum_i q_i (c_i^* - \bar{\mu}_i) - \delta \sum_i q_i c_i^* + \frac{1}{\epsilon} \sum_i U_i(c_i^*(1 - \delta)) \\
&\leq K_2 + \sum_i q_i (x_i^* - \bar{\mu}_i) - \delta \sum_i q_i x_i^*
\end{aligned}$$

where $K_2 = K - 1 + \frac{1}{\epsilon} \sum_i (U_i(\bar{c}_{max}) - U_i(\bar{c}_i^*(1 - \delta)))$

Now $\sum_i q_i \bar{c}_i^* \leq \sum_i q_i \bar{\mu}_i$,

Therefore, $E[V(q(t+1)) - V(q(t)) | q(t) = q] \leq K_2 - \delta \sum_i q_i \bar{c}_i^*$

Since δ can be any value between 0 and 1, $q(t)$ is positive recurrent according to Foster Lyapunov theorem if $c_i^* > 0$ for all i □

Chapter 6

SIMULATIONS AND RESULTS

6.1 Channel Model

A slow fading Rayleigh Channel Model is used to model the dynamics of the channel. The justification behind using a slow fading model stems from the fact that assuming a pedestrian mobile user moving at a speed of 1.7 m/s yields a coherence time of the channel that is less than an intraperiod (1s) and more than a frame timeslot (30ms). If f_m is the Doppler spread, v is the velocity and f_c the carrier frequency

$$f_m = \frac{v}{c} * f_c$$

Assuming a Carrier Frequency of 2.5Ghz we get

$$f_m = 14.667Hz \text{ and Coherence time } T_s = 60ms$$

A finite state Markov channel model is used to represent Rayleigh fading channels. The received SNR is partitioned into a finite number of states, where each state corresponds to different channel quality. The SNR at the receiver is divided into $|\mathcal{K}|$ regions using the algorithm in Zhang and Kassam (1999).

In a multipath environment the received instantaneous SNR is exponentially distributed

$$p(\lambda) = \frac{1}{\psi^{avg}} \exp\left(-\frac{\lambda}{\psi^{avg}}\right), \lambda \geq 0$$

where ψ^{avg} is the average SNR. Representative SNR for the k^{th} region $\tilde{\psi}_k$ for Rayleigh fading channels is given as

$$\tilde{\psi}_k = \frac{\int_{\psi_{k-1}}^{\psi_k} \lambda p(\lambda) d\lambda}{\int_{\psi_{k-1}}^{\psi_k} p(\lambda) d\lambda}$$

The level crossing rate, Σ which is a function of Doppler frequency f_m is given as

$$\Sigma_{\psi_k} = \sqrt{\frac{2\pi\psi_k}{\psi^{avg}}} f_m \exp\left(-\frac{\psi_k}{\psi^{avg}}\right)$$

The steady state probabilities π_i are given as

$$\pi_i = \int_{\psi_{i-1}}^{\psi_i} p(\lambda) d\lambda$$

and the Transition probability matrix is defined as

$$P_{i,j} = \begin{cases} \frac{\Sigma(\psi_j)\Delta T}{\pi_i} & \text{if } j = i + 1 \\ \frac{\Sigma(\psi_i)\Delta T}{\pi_i} & \text{if } j = i - 1 \\ 1 - \frac{\Sigma(\psi_j)\Delta T}{\pi_i} - \frac{\Sigma(\psi_i)\Delta T}{\pi_i} & \text{if } j = i \\ 0 & \text{o.w.} \end{cases}$$

In our simulations $|\mathcal{K}|=4$. The packet error rate is obtained to be

$$e_k = 1 - (1 - s_k)^{2048}$$

where symbol error rate s_k in the k^{th} SNR region, with QPSK modulation, is obtained as

$$s_k = 2Q\left(\sqrt{2\psi_k} \sin\left(\frac{\pi}{2^4}\right)\right)$$

The transmission rate

$$x_k = \frac{\Delta T}{\Delta t} L$$

where L is the packetlength for 2048 symbols (=2048*2) and the transmission time $\Delta t = 2ms$. The resultant throughput obtained is

$$x_k(1 - e_k)$$

6.2 Performance Evaluation

The performance of our user and packet scheduling algorithms were compared to heuristics proposed in Maani *et al.* (2007) (Heuristic 1) and Hassan *et al.* (2008) (Heuristic 2). The logarithm of throughput obtained by three users using heterogenous channels is plotted in Figure 6.1, 6.2 and 6.3.

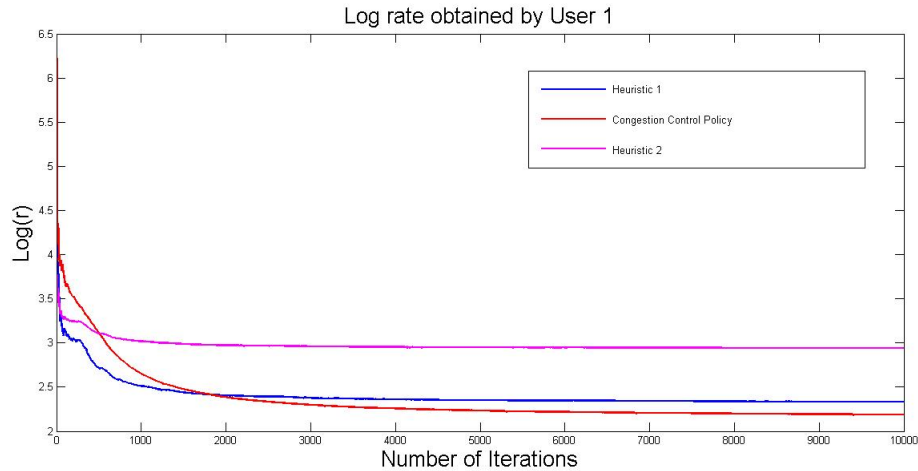


Figure 6.1: Logarithm of Throughput of User 1

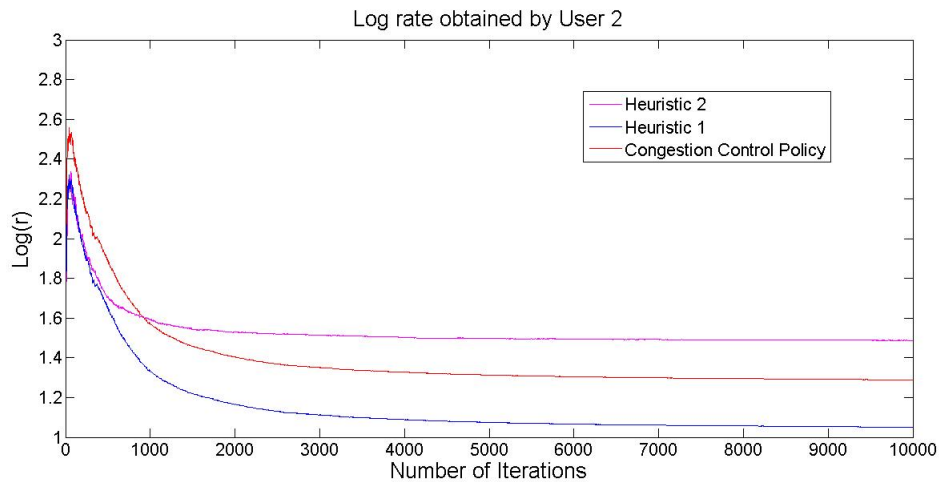


Figure 6.2: Logarithm of Throughput of User 2

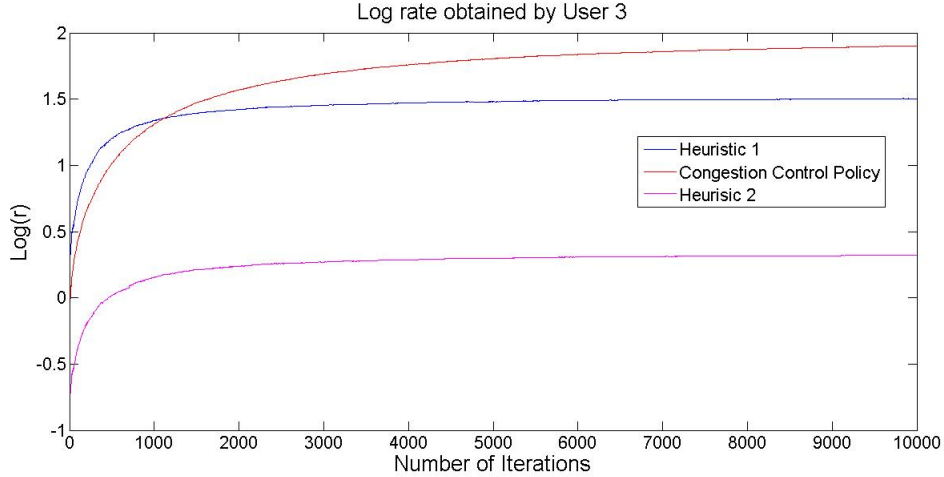


Figure 6.3: Logarithm of Throughput of User 3

In our simulations User 1 enjoys a high average throughput followed by User 2. The average throughput of User 3 is significantly lower than the throughput of the other two. Our algorithm distinctly outperforms all the others in providing a fair throughput allocation to all users, irrespective of their channel conditions. The quality obtained at the receiver end is evaluated using the MS-SSIM index proposed in Seshadrinathan *et al.* (2010). This index is further converted into a Difference Mean Opinion Score (DMOS) score by a logistic regression mechanism based on the MSSIM index and MOS value of images stored in the LIVE database. Its value ranges from 0 to 100, where 0 implies perfect visual quality and value 100 indicates the worst visual quality. The formula for conversion is as follows:

$$q^{dmos} = 13.34 \log(1 - q^{ssim}) + 3.62(1 - q^{ssim}) + 77.01$$

The DMOS scores of the policies evaluated for video coastguard.qcif is shown in the following table.

Table 6.1: DMOS Scores

Policy	User 1	User 2	User3
Congestion Control Policy	15.5956	24.8813	42.3941
Heuristic 1	15.2439	25.6421	51.6322
Heuristic 2	14.6429	24.7324	61.5721

Screenshots taken for the reconstructed video for User 3, under different algorithms are shown.



Figure 6.4: Screen shot of the reconstructed video for User 3 under Congestion Control Policy



Figure 6.5: Screen shot of the reconstructed video for User 3 under Heuristic 1



Figure 6.6: Screen shot of the reconstructed video for User 3 under Heuristic 2

Chapter 7

CONCLUSIONS AND FUTURE WORK

7.1 Conclusion

In this paper, we have proposed novel approaches for user and packet selection in wireless networks. We have derived the user selection algorithm by solving the utility optimization problem of maximizing log rates of all the users under the constraint of a fixed capacity region. For our packet scheduling algorithm, optimality was proved by showing the stability of the virtual queue and convergence of service for each of the individual users. The algorithms proposed in the thesis were tested upon real videos from the Live database and compared with other proposed schemes.

7.2 Future Work

In this thesis we have assumed that the video to be delivered is available at the server. However our model can be improved upon to include scenarios that entail live streaming, where the entire video content is not available at the server. We plan to develop similar approaches to study video conferencing for congested channels.

REFERENCES

- Chen, C., R. W. H. Jr., A. C. Bovik and G. de Veciana, “Near-optimal adaptive scheduling of scalable videos over wireless channels”, CoRR **abs/1209.2067** (2012).
- Cheng, H., X. M. Zhang, Y. Q. Shi, A. Vetro and H. Sun, “Constant quality rate allocation for fgs coding using composite r-d analysis.”, *IEEE Transactions on Multimedia* **8** (2006).
- Chou, P. A. and Z. Miao, “Rate-distortion optimized streaming of packetized media.”, *IEEE Transactions on Multimedia* **8** (2006).
- Ferrari, D. and D. C. Verma, “A scheme for real-time channel establishment in wide-area networks.”, *IEEE Journal on Selected Areas in Communications* **8**, 3, 368–379 (1990).
- Hassan, M., T. Landolsi and M. El-Tarhuni, “A fair scheduling algorithm for video transmission over wireless packet networks.”, (2008).
- Jones, G. L., “On the markov chain central limit theorem”, *Probability Surveys* **1**, 299–320 (2004).
- Lu, M.-H., P. Steenkiste and T. Chen, “A time-based adaptive retry strategy for video streaming in 802.11 wlans.”, *Wireless Communications and Mobile Computing* **7** (2007).
- Maani, E., Y. Luo, P. V. Pahalawatta and A. K. Katsaggelos, “Packet scheduling for scalable video streaming over lossy packet access networks”, (2007).
- R.Srikant and L. Ying, “Communication networks, an optimization control and stochastic networks perspective”, (2013).
- Schwarz, H., D. Marpe and T. Wiegand pp. 1103–1120 (2007).
- Seshadrinathan, K., R. Soundararajan, A. C. Bovik and L. K. Cormack, “Study of subjective and objective quality assessment of video”, *Trans. Img. Proc.* **19**, 6 (2010).
- Zhang, Q. and S. A. Kassam, “Finite-state markov model for rayleigh fading channels”, *IEEE Transactions on Communications* (1999).